Healthcare professionals using the new monitor (detector plus IF) should, therefore, have an overall proficiency in the detection and diagnosis of acute ischemia of 85% (detector sensitivity $*$ median diagnostic proficiency). We are currently conducting a clinical trial to validate the performance characteristics of the new monitor in an acute hospital setting and we are working in the integration of this monitor with the x-ray fluoroscopy imaging system used in the cardiac catheterization laboratory.

ACKNOWLEDGMENT

The authors would like to thank Prof. K. Cheah for the assistance.

REFERENCES

[1] J. S. Berger, L. Eisen, V. Nozad, J. D'Angelo, Y. Calderon, D. L. Brown, and P. Schweitzer, "Competency in electrocardiogram interpretation among internal medicine and emergency medicine residents," *Amer. J. Med.*, vol. 118, pp. 873–80, 2005.

[2] B. J. Drew, R. M. Califf, M. Funk, E. S. Kaufman, M. W. Krucoff, M. M. Laks, P. W. Macfarlane, C. Sommargren, S. Swiryn, and G. F. Van Hare, "Practice standards for electrocardiographic monitoring in hospital setting: An American Heart Association scientific statement from the councils on cardiovascular nursing, clinical cardiology, and cardiovascular disease in the young: Endorsed by the international society of computerized electrocardiology and the American Association of Critical-Care Nurses," *Circulation*, vol. 110, pp. 2721–2746, 2004.

[3] C. Papaloukas, D. I. Fotiadis, A. Likas, and L. K. Michalis, "Automated methods for ischemia detection in long-duration ECGS," *Cardiovasc. Rev. Rep.*, vol. 24, no. 6, pp. 313–320, 2003.

[4] A. Soula, Y. Kitachine, and W. Gillessen, "Method and device for representing and monitoring functional parameters of a physiological system," U.S. Patent, 2004; 6 694 178.

[5] B. Tilg, G. Fischer, R. Modre, and F. Hanser, "Model-based imaging of cardiac electrical excitation in humans," *IEEE Trans. Med. Imag.*, vol. 21, no. 9, pp. 1031–1039, Sep. 2002.

[6] J. G. Webster*, Medical Instrumentation Application and Design*, 3rd ed. New York: Wiley, 1998, ch. 6, pp. 233–264.

[7] G. Fischer, B. Tilg, P. Wach, R. Modre, and , "Application of high-order boundary elements to the electrocardiographic inverse problem," *Comp. Meth. Prog. Biomed.*, vol. 58, no. 2, pp. 119–131, 1999.

[8] J. Garcia, M. Astrom, J. Mandive, P. Laguna, and L. Sornmo, "ECG-based detection of body position changes in ischemia monitoring," *IEEE Trans. Biomed. Eng.*, vol. 50, no. 6, pp. 677–685, Jun. 2003.

[9] European Society of Cardiology, 2007 [Online]. Available: http://www.physionet.org/physiobank/database/edb/

[10] F. Jager, G. B. Moody, A. Taddei, and R. G. Mark, "Performance measurement for algorithms to detect transient ischemic ST segment changes," *Comput. Cardiol.*, pp. 369–372, 1991.

[11] N. Maglaveras, T. Stamkopoulos, C. Pappas, and M. Strintzis, "An adaptive backpropagation neural network for real-time ischemia episodes detection: Development and performance analysis using the European ST-T database," *IEEE Trans. Biomed. Eng.*, vol. 45, no. 7, pp. 805–813, Jul. 1998.

[12] J. Garcia, L. Sornmo, S. Olmos, and P. Laguna, "Automatic detection of ST-T complex changes on the ECG using filtered RMS ECG difference series: Application to ambulatory ischemia monitoring," *IEEE Trans. Biomed. Eng.*, vol. 47, no. 9, pp. 1195–1201, Sep. 2000.

[13] F. Jager, G. Moody, and R. Mark, "Detection of transient ST segment episodes during ambulatory ECG monitoring," *Comput. Biomed. Res.*, vol. 31, pp. 305–322, 1998.

[14] A. Taddei, G. Constantino, and R. Silipo, "A system for the detection of ischemic episodes in ambulatory ECG," in *Proc. IEEE Comput. Cardiol.*, 1995, pp. 705–708.

[15] S. Haggmark, M. F. Haney, S. M. Jensen, G. Johansson, and U. Naslund, "ST-segment deviations during pacing-induced increased heart rate in patients without coronary artery disease," *Clin. Physiol. Funct. Imag.*, vol. 25, pp. 246–252, 2005.

[16] J. Garcia, M. Astrom, J. Mandive, P. Laguna, and L. Sornmo, "ECG-based detection of body position changes in ischemia monitoring," *IEEE Trans. Biomed. Eng.*, vol. 50, no. 6, pp. 677–685, Jun. 2003.

A Comparison of Two- and Four-Electrode Techniques to Characterize Blood Impedance for the Frequency Range of 100 Hz to 100 MHz

Zu-yao Chang*, Gheorghe A. M. Pop, and Gerard C. M. Meijer

***Abstract*—Measurement setups that characterize the impedance of suspensions of blood over the wide frequency range of 100 Hz to 100 MHz are presented in this paper. The performance of the two- and four-electrode techniques have been compared and evaluated. By applying a combination of the two measurement techniques the best result is achieved when taking into account the main nonidealities, such as electrode polarization impedance and parasitic capacitances. It has been found that the conventional three-element model for the impedance of blood can be used for frequencies up to 1 MHz. For frequencies exceeding 1 MHz, an extended model is introduced where a constant phase angle element is used for modeling the cell membrane and a capacitor C_{liq} is added for modeling the electrical capacitance of water in blood.**

***Index Terms*—Blood impedance, cell membrane capacitance, electrical model of blood, three-element model, two- and four-electrode techniques.**

I. INTRODUCTION

BLOOD is considered to be a heterogeneous medium because of the erythrocytes in plasma. Often the electrical characteristics of suspensions of blood are modeled using the well-known three-element model of Fig. 1 [1], [2]. In this lumped model, the resistor R_p represents the electrical resistance of plasma, while the effect of the cell membrane capacitance of the erythrocytes is modeled by the capacitor C_m. Furthermore, the resistor R_i represents the effect of the interior cell resistance of the erythrocytes.

The electrical resistance R_p of blood is affected by its flow [3], [4]. Moreover, in the studies of G.A.M. Pop *et al.* [5], a remarkably strong correlation was found between the impedance components R_p and C_m of blood and the viscosity of blood. This correlation can be explained by the fact that the aggregation of erythrocytes gives rise to an increase in both the viscosity and the impedance of blood. In order to investigate the feasibility of real-time viscosity measurements that are based on electrical impedance measurements, the electrical impedance of blood has been characterized over a very wide frequency range up to frequencies f of 100 MHz. It was already reported in the studies of [6] and [7] that when the capacitor C_m (see Fig. 1) is replaced by a constant phase angle (CPA) element, the model accuracy improves significantly. However, to extract the parameter C_m or the CPA accurately, measurements over a wide frequency range are required. Performing such measurements is not an easy task. In experimental studies on blood impedance, the frequency range is usually rather limited. This is partially due to the interests in using the results for certain applications. On the other hand, this is also due to the practical constraints of making measurement setups for a wide frequency band.

Manuscript received August 2, 2006. *Asterisk indicates corresponding author.*

*Z. Chang is with the Electronic Instrumentation Laboratory, Delft University of Technology, Mekelweg 4, 2628 CD Delft, The Netherlands (e-mail: z.y.chang@tudelft.nl).

G. A. M. Pop is with the Heartcenter UMCN St. Radboud, 6500 HB, Nijmegen, The Netherlands.

G. C. M. Meijer is with the Electronic Instrumentation Laboratory, Delft University of Technology, 2628 CD Delft, The Netherlands (e-mail: z.y.chang@tudelft.nl).

Color versions of one or more of the figures in this paper are available online at http://ieeexplore.ieee.org.

Digital Object Identifier 10.1109/TBME.2008.915725

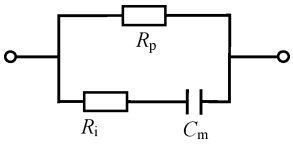

Fig. 1. Electrical model of whole blood impedance, according to [1] and [2].

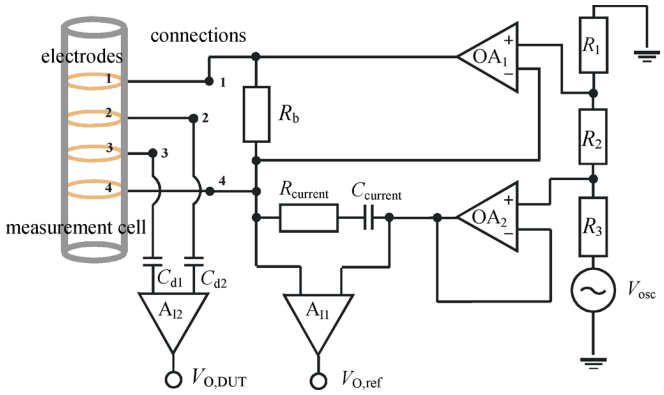

Fig. 2. Front-end measurement circuit for the four-electrode measurement setup.

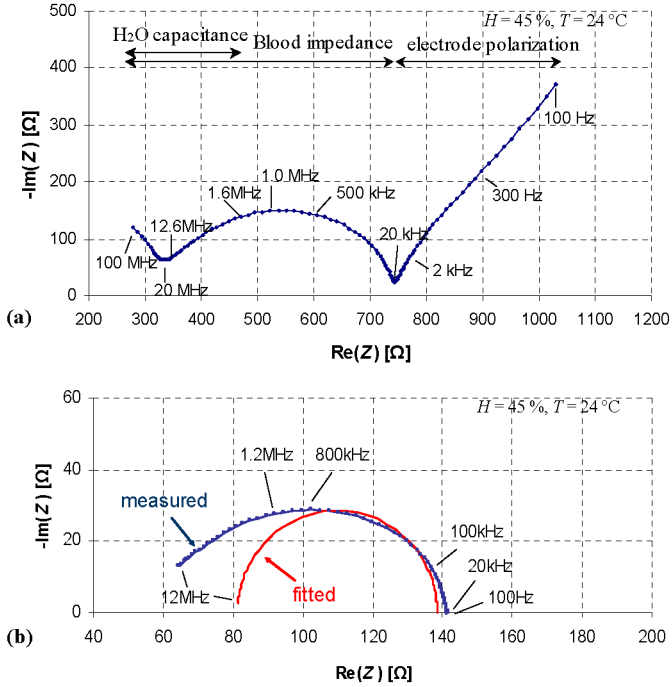

Fig. 3. (a) Nyquist plot of the measured blood impedance using the two-electrode technique. (b) Nyquist plot of the measured blood impedance using the four-electrode technique with a separate fitting curve according to the three-element model in Fig. 1.

To obtain better measurement result over a wide bandwidth, we applied a combination of two impedance measurement techniques to characterize the electrical impedance of suspensions of motionless blood. For the low-frequency range (100 Hz up to 12 MHz), a four-electrode measurement technique was applied in which the effects of polarization caused by the electrode-liquid contact were eliminated [8]. In order to reduce the amount and the effect of parasitic capacitances in the measurement setup, a two-electrode measurement technique was applied for the higher-frequency range of up to 100 MHz. Based on the measurement results, the three-element model for the electrical impedance of blood suspensions has been evaluated and an extended equivalent circuit model is proposed.

II. Measurement Setups

To measure the electrical impedance of blood, we made a cylindrical measurement cell (see Fig. 2) with four gold-ring electrodes. For the four-electrode measurement setup, a special front-end measurement circuit has been designed and implemented. In this circuit, a constant electrical current is injected via the two outer electrodes (1 and 4) of the measurement cell and the resulting voltage drop is measured with the two inner electrodes (2 and 3). The output voltages ($V_{\mathrm{O,ref}}$ and $V_{\mathrm{O,DUT}}$) are connected as input voltages for an HP4192A gain-phase analyzer to obtain the impedance results up to a frequency of 12 MHz. Because of the limited bandwidth of the amplifiers OA_1, OA_2, A_{I1} and A_{I2} and the effects of parasitic capacitances of the electrodes 3 and 4 to ground, the circuit accuracy drops significantly for frequencies higher than 12 MHz. However, by connecting the measurement cell directly to an Agilent 4294A precision impedance analyzer for the two-electrode measurement setup, the problems that occur at frequencies higher than 12 MHz can be mitigated. In that case, the amount and the effects of the remaining parasitic electrode capacitances are also reduced, which enables measurements for the wide frequency range from 100 Hz up to 100 MHz. For the wide intermediate frequencies of 20 kHz to 12 MHz both methods show equal performance.

The cylindrical measurement cell that has been used in both measurement setups has a diameter of 9.5 mm. The distance between the two inner electrodes is 3.8 mm, while the distance between the two outer electrodes is 17.8 mm. The cell constant for the four-electrode setup and the two-electrode setup are 0.54 and 2.79 cm^{-1}, respectively, where the values were extracted from the measurements of a sample with a known resistivity. By keeping the length of each of the connecting wires short (1.5 cm), the wire resistances are negligible.

From a healthy volunteer, 10 mL of blood was collected and anti-coagulated with Heparin. Next, the blood was placed in the cylindrical measurement cell. Because of the temperature dependence of blood impedance [2], [9], it was important to keep the temperature T at a constant value, which during our measurements amounted to 24 °C. In addition, to prevent the erythrocytes from settling [10] in the measurement cell, the measurements were performed immediately after a gentle shaking of the cell. We assume that shaking randomizes the distribution of the blood cells. In our experiments, the hematocrit H, which represents the volume percentage of erythrocytes in the total volume of blood, amounted to 45%.

III. Experimental Results and Characterization

The results of the two- and four-electrode measurements are shown in Fig. 3(a) and (b), respectively. Because of the geometrical differences of the electrode configurations of the two measurement setups, the values along the axis in Fig. 3(a) differ from those in Fig. 3(b). Fig. 3(a) shows that when using the two-electrode measurement technique, both the imaginary and the real part of the impedance in the frequency range 100 Hz up to 20 kHz decrease with the square root of the frequency. This is due to the polarization impedance [11], [12], which is frequency-dependent. This frequency dependency is known as α dispersion and results from the effects of the electrode-electrolyte interface. For frequencies above 20 kHz, the nonlinear effects caused by the magnitude of the applied current or voltage are minimal [13]. In Fig. 3(a), a valley can be observed for a frequency of about 20 MHz. For higher frequencies ($>$ 20 MHz), the changes in the imaginary part are similar to those of a shunting capacitance and have been identified as the effect of the electrical capacitance of water.

Fig. 3(b) shows the results of the four-electrode technique. Because of the high input impedance of the amplifier at the sense electrodes 2 and 3, the effect of the polarization impedance is eliminated. In the frequency range between 20 kHz and 12 MHz, both measurement setups

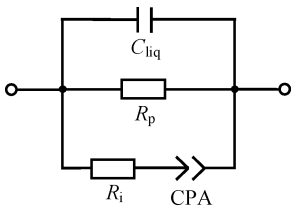

Fig. 4. Extended electrical model of whole blood impedance.

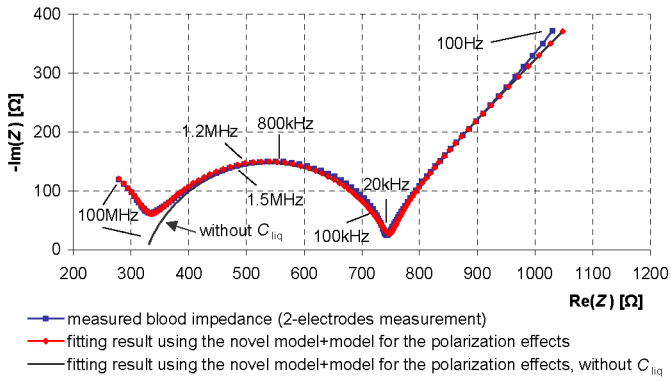

Fig. 5. Fitting results of the extended model (see Fig. 4) including the polarization effects; a simulation result for the model with $C_{\rm liq}$ omitted is also shown.

show the same characteristic, which is depicted by the depressed semi-circle. This depressed semi-circle is typical for heterogeneous media such as blood. In this frequency range, the impedance decreases as the frequency increases, which is due to the fact that at these frequencies the electrical current passes through the cell membranes of the erythrocytes. This frequency dependency is known as β dispersion.

A. Three-Element Model Fitting

A complex data-fitting program, called ZView [14], has been used to fit both the real and the imaginary parts of the measured impedance with those of the model. In Fig. 3(b), the fitting result is shown for the simple three-element model of Fig. 1. The fitting has been performed for measurement data in the frequency range from 100 Hz to 1.2 MHz and extrapolated to 12 MHz. A clear difference is that the measured impedance shows a depressed semi-circle instead of an ideal semi-circle. From the poor fitting result, we can conclude that the cell membrane cannot be well modeled with a simple capacitor C_m. Yet, for measurement frequencies below 1 MHz, an acceptable fitting accuracy can be achieved with the three-element model.

B. Extended Model for Blood Impedance

With a small extension of the three-element model of Fig. 1, it is possible to improve the performance of the model. First, instead of using a capacitor C_m to model the cell membrane capacitance, a CPA element can be used, as proposed in [6] and [7]. This CPA element has an impedance $Z_{\rm CPA}$, which equals

$$Z_{\rm CPA} = \frac{1}{(j\,\omega)^{\alpha} C} \tag{1}$$

where C is a constant, $\omega = 2\pi f$, and $0 < \alpha < 1$.

Next, in the model a capacitor $C_{\rm liq}$ is placed parallel to the three-element model. This capacitance models the dielectric capacitance of the intra-cellular and extra-cellular fluid of blood, which mainly consists of water. The effects of both extensions are shown in Fig. 4, which displays the extended electrical model of blood. Combining the extended electrical model of blood with the model in [11] for the polarization impedance, results in a fitting graph that is shown in Fig. 5. From the excellent fitting results, we can conclude that we have a good model for the electrical impedance of blood for frequencies up to 100 MHz. In the simulations, the influence of the electrical capacitance of water $C_{\rm liq}$ can easily be shown. The non-dotted line in Fig. 5 shows the simulated impedance result for the case that $C_{\rm liq}$ hasbeen omitted.

IV. Conclusion

It has been shown that for an accurate characterization of blood impedance over a wide frequency range, a combination of two measurement techniques yields the best performance. For the low-frequency range (100 Hz up to 20 kHz) the four-electrode technique is most useful, while for the higher frequency range (12 to 100 MHz) the two-electrode technique gives the better performance. For the intermediate range, both techniques give a similar performance.

The traditional three-element model (R_p, R_i and C_m) for the impedance of suspensions of blood can be used for a frequency range up to 1 MHz. For higher frequencies up to 100 MHz, an extended model is proposed. In this model, the capacitor C_m is replaced by a so-called CPA element, and a shunting capacitor $C_{\rm liq}$ is added simultaneously. The capacitor $C_{\rm liq}$ represents the electrical capacitance of water in blood, which has an influence at frequencies from 1.5 MHz onwards.

References

[1] H. Fricke, "The electrical resistance and capacity of blood for frequencies between 800 and 4.5 million cycles," *J. Gen. Phys.*, vol. 9, p. 153, 1925–1926.

[2] T. Zhao and B. Jacobson, "Triple-frequency method for measuring blood impedance," *Physiology Measurements*, vol. 14, pp. 145–156, 1993.

[3] Sigman *et al.*, "Effect of motion on the electrical conductivity of blood," *Amer. J. Phys.*, vol. 118, pp. 708–719, 1937.

[4] G. A. Pop, Z. Chang, C. J. Slager, B. Kooij, E. D. van Deel, L. Moraru, J. Quak, G. C. Meijer, and D. J. Duncker, "Catheter-based impedance measurements in the right atrium for continuously monitoring hematocrit and estimating blood viscosity changes; An in vivo feasibility study in swine," *Biosen. Bioelect.*, vol. 19, no. 12, pp. 1685–1693, Jul. 2004.

[5] G. A. M. Pop, W. J. Hop, M. van der Jagt, J. Quak, D. Dekkers, Z. Chang, F. J. Gijsen, D. J. Dunncker, and C. J. Slager, "Blood electrical impedance closely matches whole blood viscosity as parameter of hemorheology and inflammation," *Appl. Rheol.*, vol. 13, no. 6, pp. 305–312, 2003.

[6] J. Z. Bao, C. C. Davis, and R. E. Schmukler, "Frequency domain impedance measurements of erythrocytes. Constant phase angle impedance characteristics and a phase transition," *Biophys. J.*, vol. 61, no. 5, pp. 1427–1434, May 1992.

[7] Y. Ulgen and M. Sezdi, "Electrical parameters of human blood," in *IEEE Eng. Med. Biol. Soc.*, 1998, pp. 2983–2986.

[8] H. P. Schwan, "Electrode polarization impedance and measurements in biological materials," *Ann. NY Acad. Sci.*, vol. 148, no. 1, pp. 191–209, 1968.

[9] F. Jaspard and M. Nadi, "Dielectric properties of blood: An investigation of temperature dependence," *Phys. Meas.*, vol. 23, pp. 547–554, 2002.

[10] T. Zhao and D. Lockner, "Electrical impedance and erythrocyte sedimentation rate (ESR) of blood," *Biochim. Biophys. Acta.*, vol. 1153, pp. 243–248, 1993.

[11] E. T. McAdams, A. Lackermeier, J. A. McLaughlin, D. Macken, and J. Jossinet, "The linear and non-linear electrical properties of the electrode-electrolyte interface," *Biosen. Bioelect.*, vol. 10, pp. 67–74, 1995.

[12] J. R. Macdonald, Ed., Impedance Spectroscopy; Emphasizing Solid Materials and Systems New York, Wiley, 1987, pp. 23, 64–103.

[13] L. A. Geddes and C. Sadler, *Principle of Applied Biomedical Instrumentation*, 3rd ed. New York: Wiley, 1989, pp. 332–339.

[14] Scribner Associates, Inc., Southern Pines, NC, "ZPlot/ZView," 1980 [Online]. Available: http://scribner.com /products/zplot/